Global Scientific JOURNALS

GSJ: Volume 11, Issue 5, May 2023, Online: ISSN 2320-9186
www.globalscientificjournal.com

MEASUREMENT OF DOUBLE LAYER CAPACITANCE AT BISMUTH BULK ELECTRODES (BiBEs) IN AQUEOUS SOLVENTS

Aondoakaa S. Nomor [1,2] and Ben. R. Horrocks [1]

1. School of Chemistry, Bedson Building, Newcastle University
   Newcastle upon Tyne, NE1 7RU, UK
   E-mail: ben.horrocks@ncl.ac.uk
2. Department of Chemistry
   Benue State University
   Makurdi, Nigeria
   E-mail: snomor@bsum.edu.ng; nomorsteve@gmail.com

1. Abstract

Bismuth bulk electrodes (BiBEs) have been suggested as possible replacements for mercury electrodes in electroanalytical studies in part because they are simply prepared by melting bismuth powder in a glass capillary and also because of the relative lack of toxicity of Bi. The double layer of BiBEs in aqueous media was studied using electrochemical impedance spectroscopy. The differential capacitance of BiBEs was determined in three aqueous electrolytes: sodium nitrate, sodium bromide and sodium chloride. Comparative measurements were made with a polycrystalline platinum electrode. Up to 43 μF cm^{-2} were recorded for the double layer capacitance at the BiBEs in the aqueous electrolytes. Combined investigations by EIS and x-ray photoelectron spectroscopy (XPS) suggest the high values of capacitance in the aqueous electrolytes are due to pseudocapacitance effects, owing to adsorptions of bromide and chloride ions as well as the formation/reduction of a bismuth(III) oxide film at the electrode surface. The EIS measurements also enabled the determination of the potential of zero charge PZC of -0.49 V versus Ag/AgCl at BiBEs in the aqueous electrolyte mixture of $NaNO_3$/NaCl. From these results, it can be concluded that electrochemical measurements at bismuth could be reproducible, and that the irregular variation of capacitance with concentration is only a confirmation that the bismuth electrode surface is not an ideal capacitor.

Keywords: Bismuth bulk electrodes, double layer capacitance, aqueous electrolytes, electrochemical impedance spectroscopy, x-ray photoelectron spectroscopy.

2. Introduction

In the search for an electrode material that will replace mercury in electroanalysis, research has centred on bismuth owing largely to its reputation as benign to the environment and to many species.[1-8] A number of factors account for the environmental friendliness of bismuth. These include its extremely low toxicity compared to mercury and widespread pharmaceutical use. It can also form multicomponent, low melting temperature alloys with numerous heavy metals.[1, 4, 7, 8] Other features of bismuth electrodes that are favourable for its use as an electrode material include low cost and ease of fabrication because of the relatively low melting point of the semi-metal as well as relative insensitivity to dissolved oxygen in aqueous solutions by comparison with mercury.[4, 5, 9, 10]

Bismuth electrodes can be broadly classified into bismuth bulk electrodes (BiBEs)[11-13] and bismuth film electrodes (BiFEs).[14-16] Factors that are responsible for the differences between bismuth bulk and film electrodes include surface roughness or morphology[12] and the substrate[1] that forms the support for the electrode material. Whereas bismuth bulk electrodes are essentially made of polycrystalline bismuth, bismuth film electrodes constitute of a thin film of Bi(III) ions; by their *in situ* reduction and deposition over a substrate such as glassy carbon or carbon paste.[1, 6, 10] Other carbon substrates used in bismuth film electrodes include pencil-lead, wax impregnated graphite and screen-printed carbon ink.[17] The conductivity of polycrystalline bismuth is lower than that of glassy carbon used as substrate in BiFEs.[12] Consequently, BiBEs may exhibit lower responses than BiFEs. The low activity of BiBEs in electrochemical processes has also been attributed to their relatively low density of states (DOS); the carrier density is of the order of 3×10^{17} cm^{-3} eV^{-1} while that of platinum, a typical metal is 1.2×10^{23} cm^{-3} eV^{-1}. [18-20] This carrier density is typical of a semi-metal.[20] In a semi-metal, one band is almost filled and another almost empty, e.g., as a result

of the conduction edge being slightly lower than the valence band edge. The small overlap of the conduction and valence bands leads to a small density of states near the Fermi level and a small carrier density. Another implication of the small overlap of the conduction and valence bands is that, high energy electrons in the valence band can enter into the conduction band without excitation. If energy is supplied in the form of heat, more valence electrons will move to the conduction band, hence increase in conductivity.

This partly explains the lower electroactivity of bismuth bulk electrodes compared to the noble metal electrodes and to bismuth film electrodes with glassy carbon as substrate. However, it should be noted that the surface of elemental Bi has different properties from the bulk and there is evidence that the carrier density at the surface of BiBEs is comparable to metal electrodes.[19]

Bismuth bulk electrodes also have a very wide potential window in alkaline media: as large as -0.47 V to -1.70 V in 0.1 M NaOH has been reported.[12] The smooth surface of BiBEs can also be easily regenerated by polishing.[1]

One major shortcoming of BiBEs however lies in their oxidation at high positive potentials[10, 12], although in compensation, their operational potential window usually extends towards more negative potentials than common electrode materials such as Pt, Au and C.

The aim of this study was to establish the use of bismuth electrodes as a potential replacement for mercury in electroanalysis. One of the steps taken to achieve this was to carry out impedance measurements in selected aqueous and non-aqueous solvents at bismuth. The results of differential capacitance obtained from the measurements were compared with those obtained at platinum, a noble metal electrode, since neither the dropping mercury electrode (DME) nor the hanging mercury drop electrode (HMDE) was used in the investigation.

3. Materials and methods

Materials

Bismuth powder (>99.999%) of particle size 150 μm was obtained from Goodfellow Cambridge Limited, England. Sodium nitrate ($NaNO_3$) and sodium bromide (NaBr) were purchased from BDH Limited Poole, England while sodium chloride (NaCl) was obtained from Alfa Aesar,

Lancaster, UK. Acetonitrile, CH_3CN (AN) and lithium perchlorate, $LiClO_4$ used in this research are products of Sigma Aldrich, Gillingham, UK

Platinum (Pt) was also used as working electrode (WE) to compare output of results at such a noble metal electrode with that of bismuth, in which case, gold disc electrode of outer diameter (OD) 6 mm and internal diameter (ID) 3 mm was used as the counter electrode (CE). Platinum disc electrodes, also of OD 6 mm and ID 3 mm and platinum wire were however mainly used as counter electrodes when Bi was used as WE. The non-aqueous $Ag/AgNO_3$ (0.01 M) reference (IJ Cambria, UK) was accordingly used for analysis in the $AN/LiClO_4$ electrolyte mixture. The surface area of the 3 mm gold and platinum electrodes was 0.071 cm^2.

High purity (99.99%) Ag wire of diameter 0.5 mm, purchased from Goodfellow Limited, Cambridge, England was used as reference in an experiment to trace the sources of peaks observed in the capacitance-potential curves at bismuth. X-ray photoelectron spectroscopy was used to confirm source of the peaks.

Nanopure water used in this research was obtained from a Barnstead Nanopure™ purification train (model DH 931, Barnstead International, Dubuque, Iowa, USA) with nominal 18.2 MΩ cm resistivity. All the reagents were used as received without further purification.

Preparation of reagents

Capacitance measurements were conducted separately in pure aq. $NaNO_3$ solutions and in NaCl as supporting electrolyte. In each case, 100 mM concentration of the salt (molar mass 84.99 g mol^{-1}) was prepared by dissolving 2.1248 g in 250 mL of solution. Nanopure water was used as electrolyte in one case while 0.1 M NaCl was used as supporting electrolyte in the other whence lower concentrations of 50 mM, 30 mM and 10 mM were obtained from the stock by dilution with the supporting electrolyte.

Similarly, 100 mM NaCl was prepared by dissolving 5.844 g of the salt (molar mass 58.44 g) in enough of nanopure water to give 1000 mL of solution. Lower concentrations of 50 mM, 30 mM and 10 mM were obtained by dilution to 250 mL volumes.

A similar approach was adopted for the preparation of NaBr electrolyte solutions. 2.5725 g of the salt whose molar mass is 102.9 g mol^{-1} was dissolved in enough of nanopure water in a 250 mL volumetric flask to give a 100 mM solution. Lower concentrations of 50 mM, 30 mm and 10 mM were obtained by serial dilution in flasks of the same capacity with nanopure water. For lithium perchlorate $LiClO_4$, 2.6597 g of the salt of molar mass 106.39 g mol^{-1} was dissolved in enough of acetonitrile CH_3CN (AN), to give a 100 mM concentration in 250 mL of solution. Lower concentrations of 50 mM, 30 mM and 10 mM were equally obtained by dilution of the stock using AN as supporting electrolyte.

Construction of Bismuth Electrodes

A soda-lime glass capillary of length 13 cm, 6 mm outer diameter and 1.92 mm bore (internal diameter) was sealed at one end in a blue flame. The cooled capillary was then filled with pure bismuth powder to about 3 cm of the glass length through the open end by means of an injection needle. Copper wire of diameter 1.13 mm was inserted into the soda-lime glass and made to penetrate 1 cm into the bismuth powder. The powder was then melted under vacuum by heating the sealed end of the capillary tube as the open end was connected to a vacuum pump. The aim of melting under vacuum was to avoid oxidation of the bismuth, after which the glass was cooled to room temperature.

The sealed end of the glass capillary was finally ground to provide a smooth surface, extreme care being taken to ensure that the copper wire was not exposed at the surface. The open end was glued with epoxy resin to prevent the copper wire from becoming loose due to mechanical stress when the electrode is connected to an external circuit. From the dimensions of the soda-lime glass, the surface area of the bismuth electrode was calculated to be 0.029 cm^2. The surface areas of the working electrodes of bismuth and platinum were used in computing the capacitance values.

Capacitance measurements

Capacitance data were obtained at the Bi|solution interface for the aqueous electrolyte solutions of $NaNO_3$, NaBr and NaCl. Impedance (potential scan) measurements were made at various dc potential ranges in the concentration range of 10 mM to 100 mM but at fixed frequencies of 500

Hz, 1000 Hz and 2000 Hz for each concentration of analyte so as to check the effects of these parameters on the charge storage capacity of the bismuth electrode. The measurements were made using an Ivium compactstat model e 1030 (±10 V/±30 mA) (Ivium Technologies, The Netherlands) connected to a Dell Precision workstation.

All the experiments were performed in a standard three-electrode cell containing 18-20 mL of sample solution. The Bi electrode served as the WE and except where comparison of output was desired, a Pt disc electrode was used. The reference electrode was Ag/AgCl (1 M KCl(aq)).

The electrochemical cell was purged with a stream of argon gas for about 8-10 minutes prior to every experimental run to remove traces of oxygen that may otherwise interfere with the electrode reactions.[21-23] After each analysis, the working electrode was polished with a slurry of 0.05 μm alumina powder of Banner Scientific Ltd., Coventry, UK spread over an 8 inch Buehler microcloth surface and thereafter, rinsed with nanopure water.

X-ray Photoelectron Spectroscopy (XPS)

A Kratos Axis Ultra 165 photoelectron spectrometer equipped with a monochromatic Al Ka X-ray excitation source (1486.7 eV) with an operating power of 150 W (15 kV, 10 mA) (NEXUS, Newcastle University) was used to collect photoemission spectra (NEXUS, Newcastle University). The binding energies obtained from the XPS analysis were calibrated using the lowest C1s component (284.6 eV) as reference from the CasaXPS baseline data. Spectral peaks were fitted using the WinSpec program developed by LISE laboratory, Universitaires Notre-Dame de la Paix, Namur, Belgium.

4. Results and Discussion

Capacitance measurements at bismuth in aqueous solutions

Results of the measurements for the Bi-$NaNO_3$ interphase are presented in figure 1. The values of differential capacitance, plotted against potential were obtained from equation (1) in which *f* stands for the frequency of measurement and *Z''* is the imaginary part of the electrochemical impedance, the surface area of the electrode factored in to obtain a value with units of μF cm^{-2}.

$$C = \frac{-1}{2\pi f Z''} \quad (1)$$

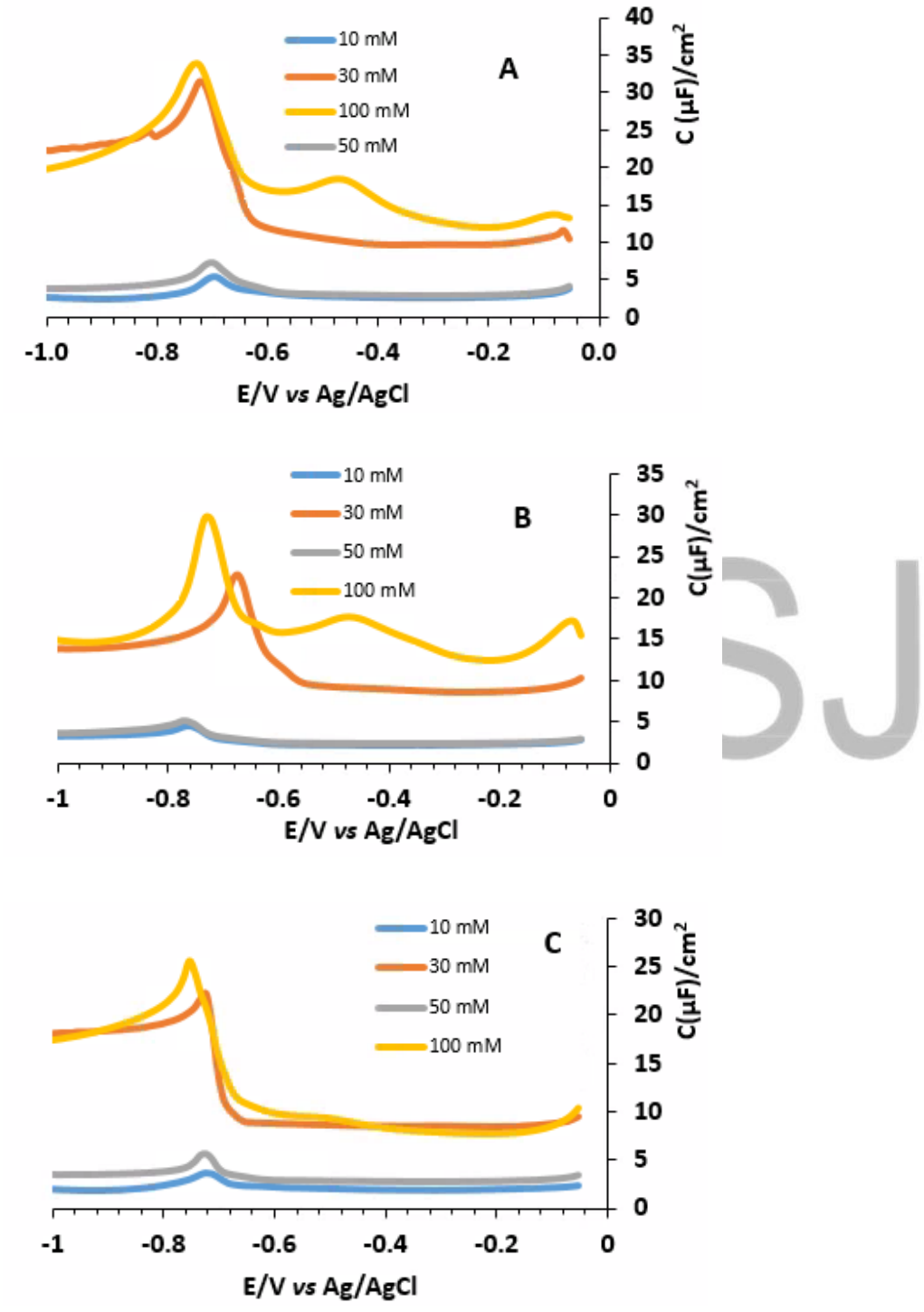

Fig. 1. Capacitance – potential data at Bi in aq. $NaNO_3$ at (A) 500 Hz (B) 1 kHz (C) 2 kHz

These results clearly show that the capacitance-potential (C_d – E) curves for the Bi|$NaNO_3$ interface are maximum values at all the frequencies (500 Hz, 1 kHz and 2 kHz) and electrolyte concentrations (10, 30, 50 and 100 mM) investigated. These measured capacitance values are not quite in agreement with the frequency independence expected from equation (1) as they tend to decrease slightly with increase in applied frequency. This is typical of constant phase element (CPE) behaviour where the phase angle is not expected to change with frequency. The maxima in the capacitance-potential curves also suggest failure of the Gouy-Chapman model for the Bi|aqueous electrolyte interphase, which predicts a minimum in the dependence of capacitance on applied potential. Electrocapillary maxima (ECM) are characteristic of surface tension-potential plots[21-23] in which the potential of zero charge, PZC is estimated from the gradient of the slope. Estimation of PZC at the bismuth electrode surface therefore becomes difficult in this instance.

Capacitance measurements were also carried out in aqueous electrolyte solutions of sodium bromide (NaBr) and sodium chloride (NaCl). The capacitance-potential data obtained showed similarities to that obtained at bismuth in sodium nitrate, with maximum values of capacitance. Apart from a few cases of irregular behaviour, the variation of capacitance with concentration follows theoretical prediction as values generally increase with increase in concentration of the analyte solution. The mathematical expression for this prediction is

$$C_d = 228zC^{\frac{1}{2}}\cosh(19.5z\varphi_0) \qquad (2)$$

In equation (2), C_d is the differential capacitance in μF cm^{-2}, *C* is the bulk concentration in mol dm^{-3}, *z* is the charge of the ions and φ_o is the total potential drop across the solution side of the double layer. In essence, the capacitance of the diffuse layer increases with concentration of ions because the average distance, as measured by the Debye length, between the counter charges and the electrode decreases. The results of the capacitance measurements at the bismuth electrode surface can therefore be said to consistent with general expectations. The capacitance-potential data in NaBr are presented in figure 2 while that obtained in NaCl are presented in figure 3.

The maxima in the capacitance-potential curves in the Bi|NaBr and Bi|NaCl interphases have been attributed to adsorptions of bromide and chloride ions at the bismuth electrode surface.[13, 24, 25] While the source of these high values of differential capacitance could be traced to adsorptions

of the halide anions on the electrode surface, the peaks characteristic of the Bi|$NaNO_3$ could not be easily accounted for.

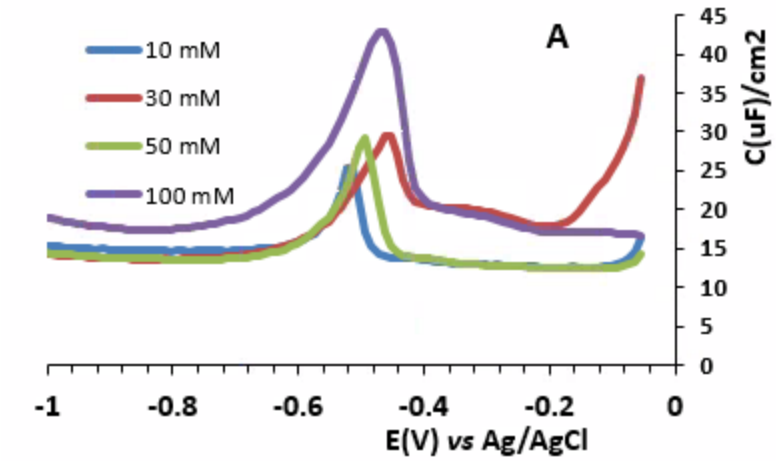

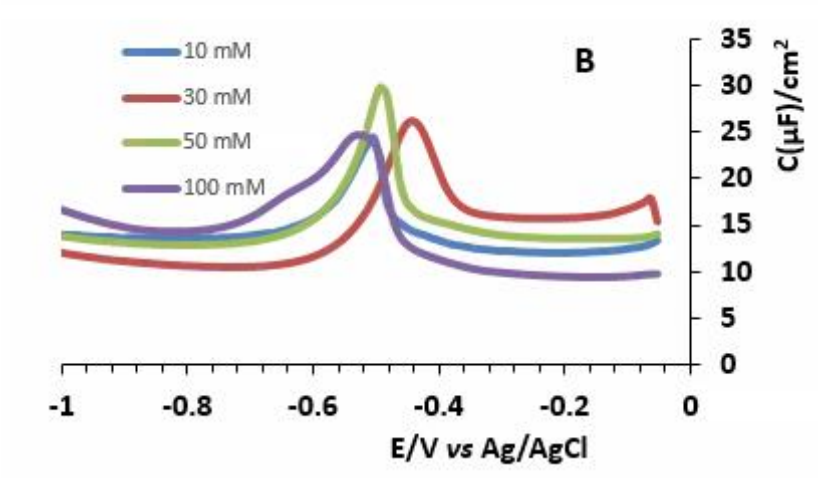

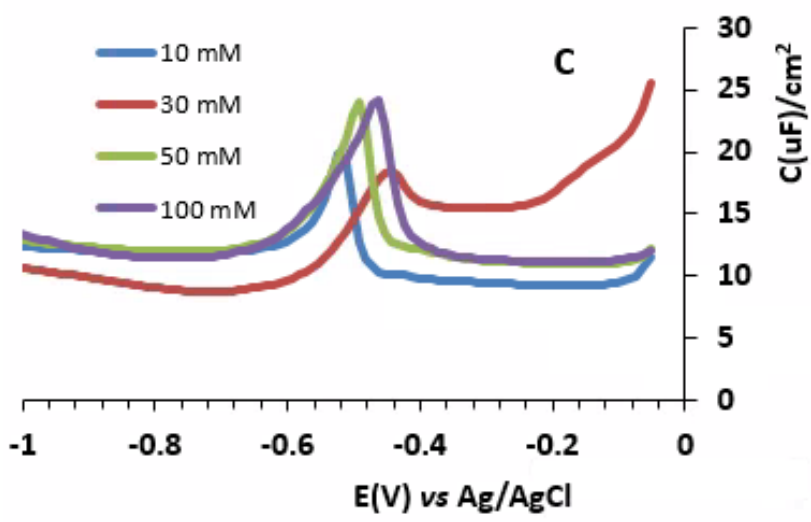

Fig. 2. Capacitance – potential data at Bi in aq. NaBr at (A) 500 Hz (B) 1 kHz (C) 2 kHz

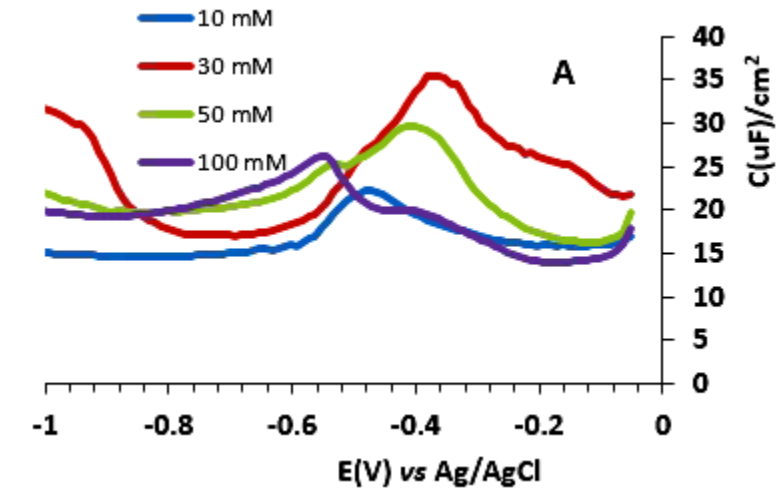

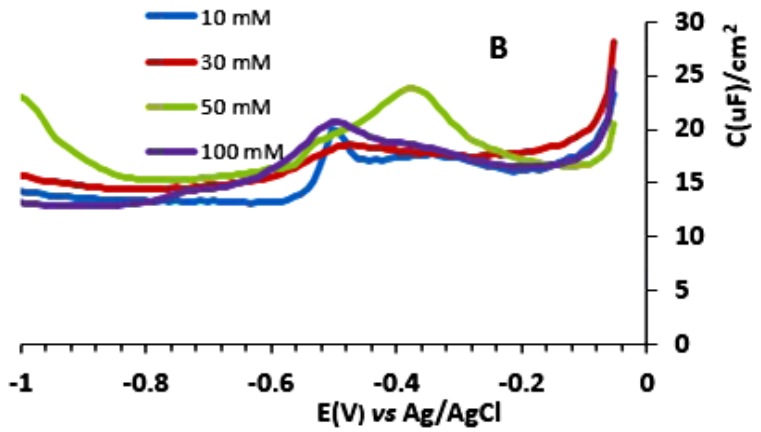

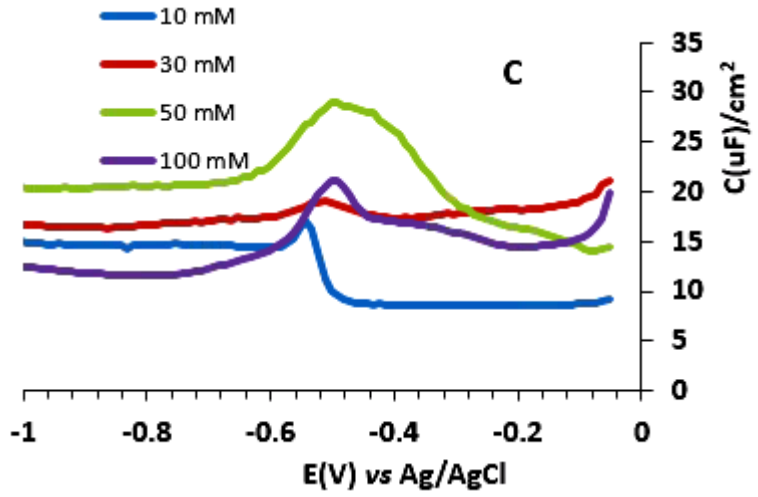

Fig. 3. Capacitance – potential at Bi in aq. NaCl at (A) 500 Hz (B) 1 kHz (C) 2 kHz

To eliminate the possibility of chloride ion Cl^- interference by leaching into the $NaNO_3$ from the Ag/AgCl reference electrode, separate experiments were conducted, but with pure Ag wire as the reference electrode (RE). Capacitance-potential data obtained at bismuth in aqueous $NaNO_3$ with Ag wire as reference are presented in figure 4.

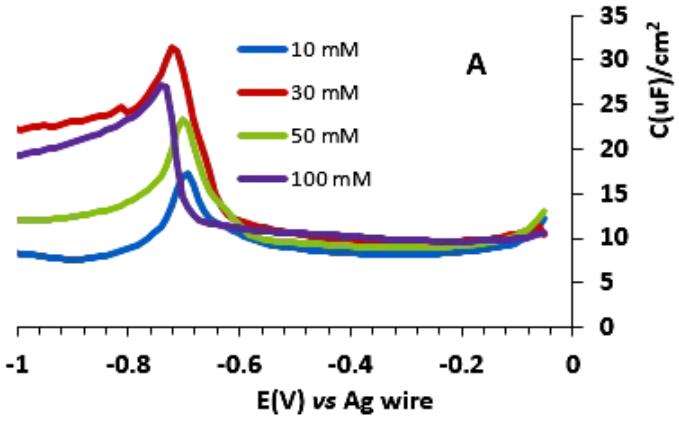

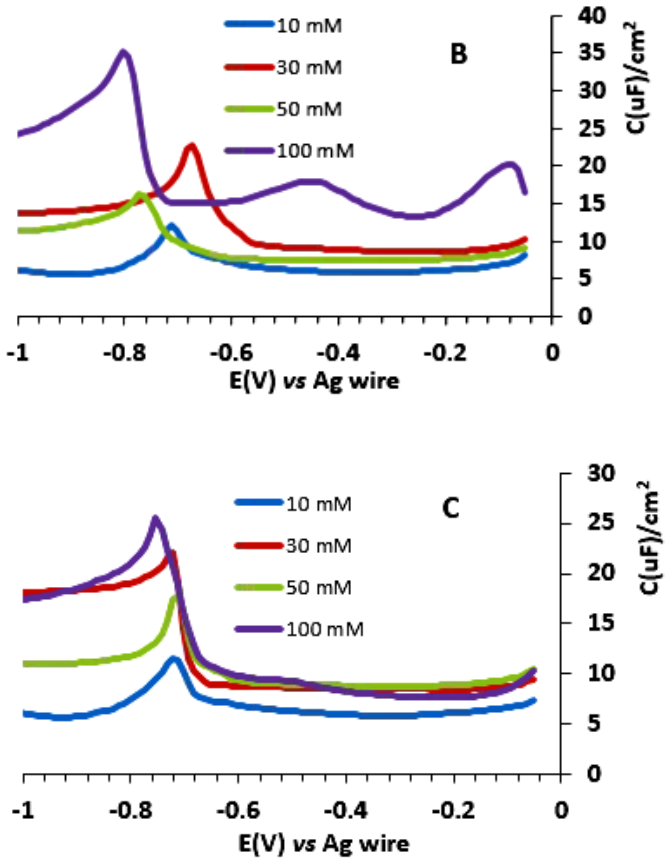

Fig. 4. Capacitance data with Ag wire as RE at Bi in aq. $NaNO_3$ at (A) 500 Hz (B) 1 kHz (C) 2 kHz

The results showed a shift in the capacitance maxima at potentials of about -0.5 V to more negative values of about -0.7 V *vs* Ag wire, but no other substantial change. This indicates a simple shift of the potential scale on changing the reference and not an effect due the Cl^-.The influence of negative potential was exerted more on the 100 mM concentration of the analyte where a value of -0.793 V was recorded at the frequency of 1 kHz.

As differential capacitance measurements alone were not sufficient to probe the Bi|electrolyte interphase, X – ray photoelectron (XPS) spectroscopy measurements were carried to ascertain the source of the peaks. These data are presented in figure 5.

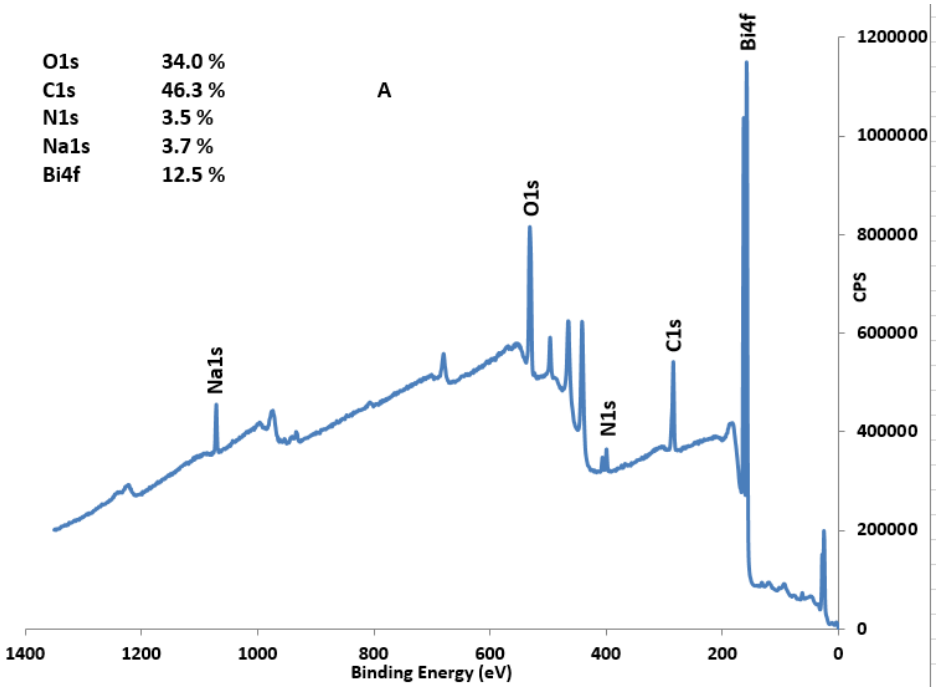

Fig. 5 (A). XPS survey spectrum of the Bi|$NaNO_3$ interphase.

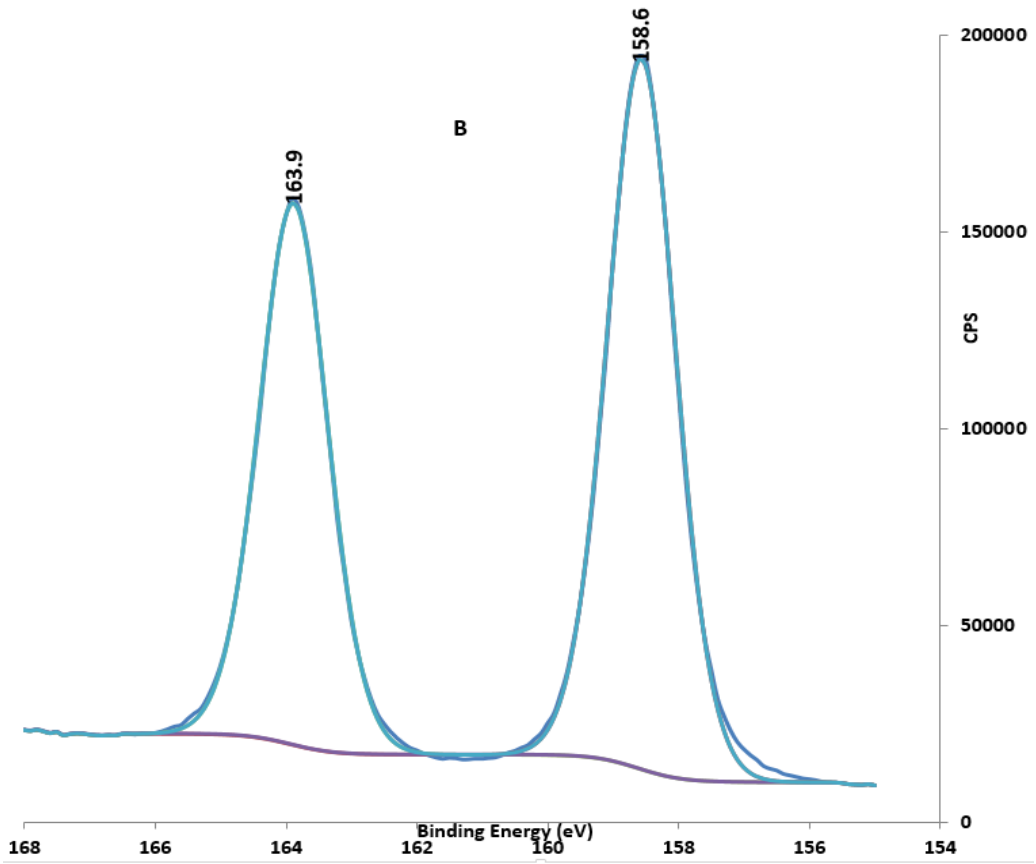

Fig. 5(B). XPS resolution spectrum of the B|$NaNO_3$ interphase.

The XPS survey and resolution spectra of all the analyte concentrations of $NaNO_3$ indicated an abundance of bismuth in the 4f spectral line. The experimental values of lower binding energy (B.E) of 158.6 eV but higher stability for 4f7/2 has been found to be due to bismuth metal[26-34] while the higher B.E of 159.3 eV also of the 4f7/2 spectral line and 163.9 eV for 4f5/2 are characteristic of bismuth(III) oxide (Bi_2O_3) and O_2/Bi adsorption[34-39], respectively. The spin-orbit splitting of these bismuth peaks is in the intensity ratio of 4:3. XPS spectra affirming the presence of peaks due to adsorption of Cl^- in the Bi|NaCl interphase have been discussed elsewhere.[40]

The double electrolyte effect

Sodium nitrate is itself an electrolyte, but to further investigate into the adsorption behaviour of the nitrate ion, the salt was prepared in aqueous sodium chloride solution as supporting electrolyte. The output of data at the frequency of 1 kHz, presented in figure 6 yielded curves with minimum values from which the potential of zero charge, PZC was estimated to have a value of -0.49 V. Herein lies the significance of the $NaNO_3$/NaCl electrolyte mixture.

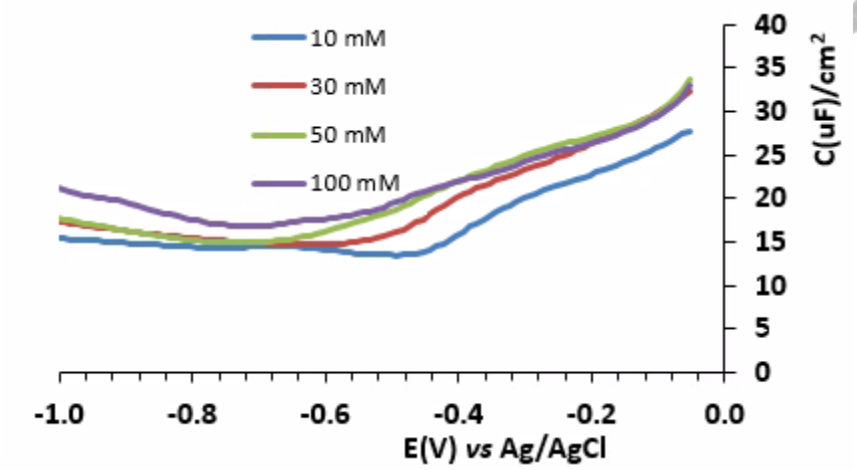

Fig. 6. Capacitance at Bi in the $NaNO_3$/NaCl electrolyte mixture at 1 kHz showing a pzc of -0.49 V.

Capacitance measurements at platinum in aqueous solutions

Electrochemical impedance spectroscopy measurements were also performed at platinum disc electrodes in the aqueous solutions of NaBr and NaCl, the electrolytes with halide ions whose adsorption at the bismuth electrode surface have been confirmed, with the Ag/AgCl electrode as reference. In contrast to the data obtained at bismuth, the capacitance-potential curves resulting from these experiments had minimum values at all analyte concentrations and frequencies of measurement, i.e., they behave much more in line with expectations from the double layer theories. This output is strongly linked to the relatively higher density of states (DOS), characteristic of a noble metal as compared to the lower carrier density of a semi-metal such as bismuth. The set of data acquired at Pt in NaBr(aq) are as presented in figure 7. It can be observed from the data that, values of double layer capacitance decrease with increase in frequency as predicted by equation (1). The potential of zero charge, PZC at Pt could be estimated from the mean of the minimum values at all the frequencies to be -0.32 V with respect to the Pt|NaBr interface.

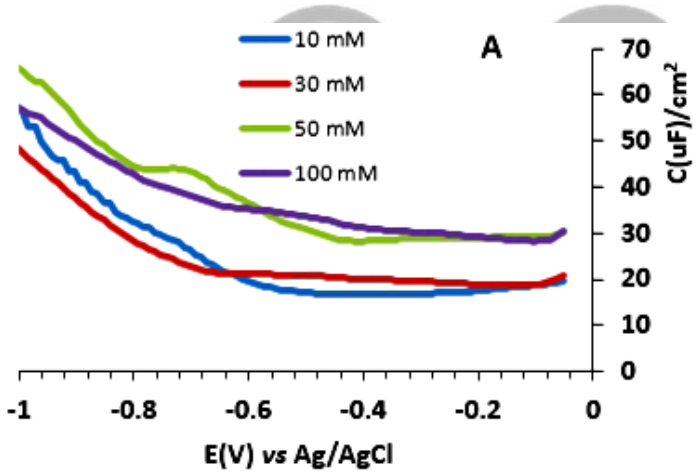

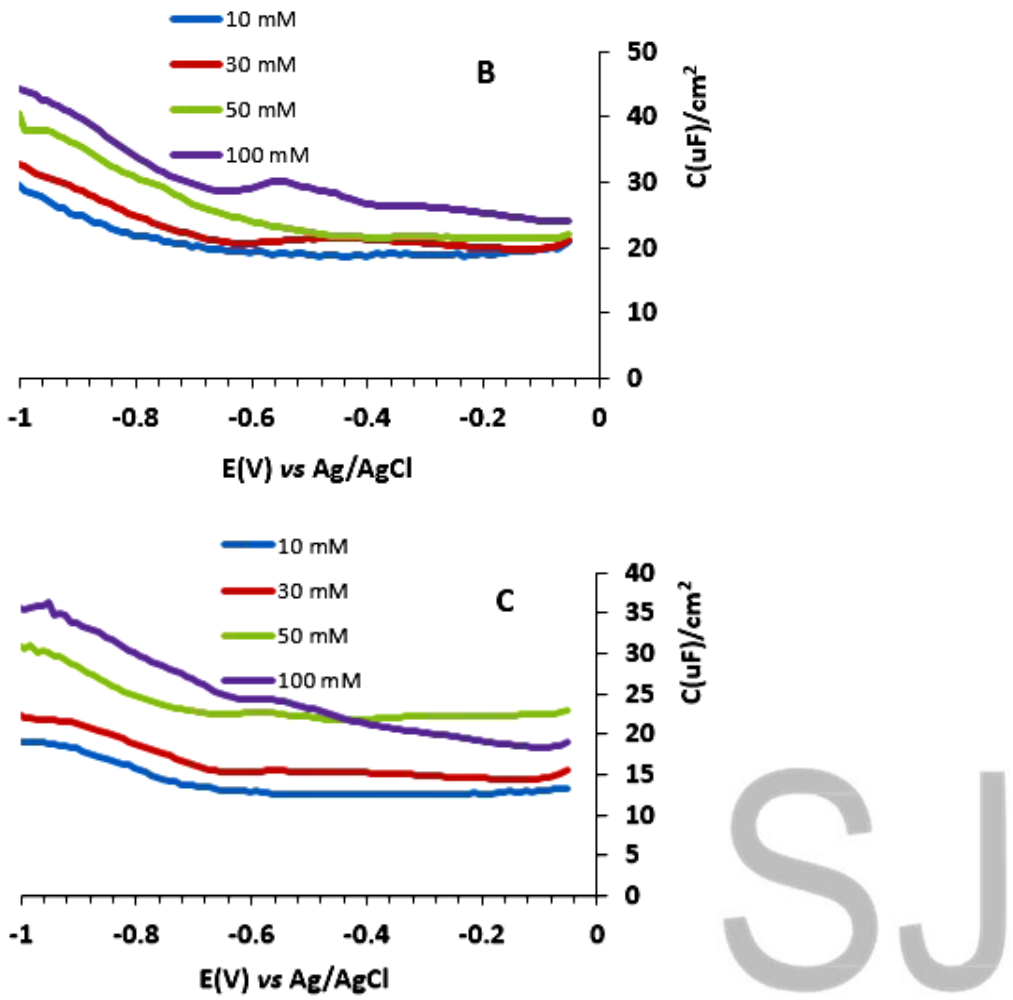

Fig. 7. Capacitance data at Pt in aq. NaBr at (A) 500 Hz (B) 1 kHz (C) 2 kHz

The capacitance-potential data curves at Pt in aqueous NaCl show semblance with those obtained in NaBr electrolyte solution in terms of decrease with frequency as observed in figure 8. In

addition, increase in capacitance with concentration is reflected in this electrolyte.

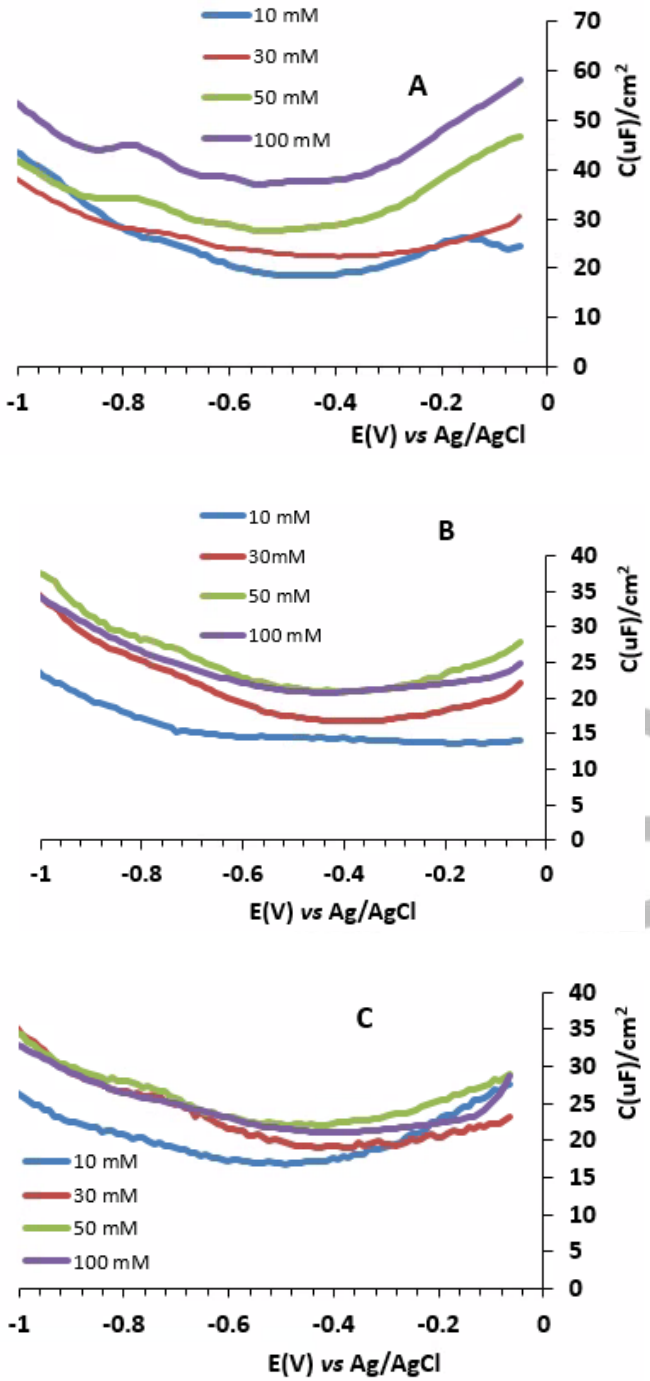

Fig. 8. Capacitance data at Pt in aq. NaCl at (A) 500 Hz (B) 1 kHz (C) 2 kHz

Capacitance measurements at bismuth in non-aqueous solvents

The charge storage capacity of the bismuth electrode surface was also investigated in the non-aqueous electrolyte mixture of acetonitrile (AN) and lithium perchlorate. While the former is adjudged to be an excellent polar organic solvent and ideal for analysis owing to its relatively high dielectric constant and dipole moment, the latter is a very good inorganic electrolyte that ionizes completely in solution. Acetonitrile has a dipole moment of 3.44 D and a dielectric constant of 37.5 at 20 ℃.[41] This value of dielectric constant, considered to be high in some circumstances is still lower than that of water which is 80.1 at the same temperature of 20 ℃.

As can be clearly observed from figure 9, all values of double layer capacitance of the bismuth - acetonitrile (AN) interphase lie below 20 µF cm^{-2} at the three frequencies of measurement. The very low capacitance of the Bi|AN interphase could be attributable to the relatively low dielectric constant of acetonitrile[13] as well as the weak adsorption of the ClO_4^- at the bismuth electrode surface.[42] Lithium perchlorate $LiClO_4$ is believed to exhibit low surface activity in non-aqueous solutions. An un-usual behaviour of the bismuth electrode in these non-aqueous solvents is the steady decrease of stored charge as the concentration of analyte increases. This could be due to increased surface activity of lithium perchlorate as the concentration increases.

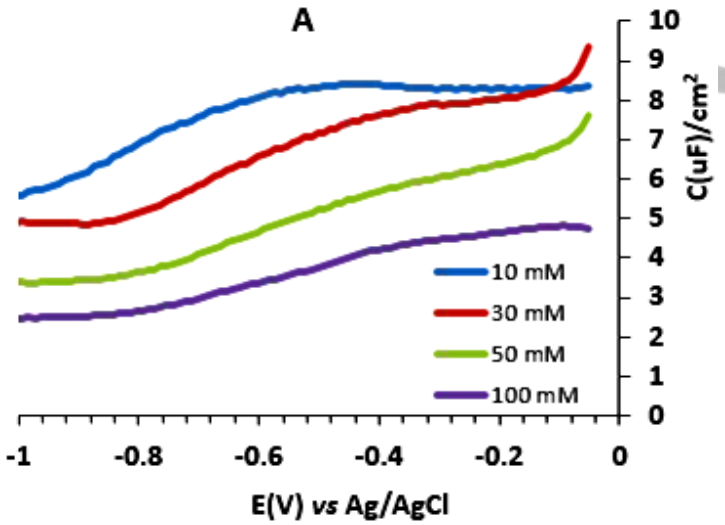

Fig. 9 (A). Capacitance data at Bi in the non-aqueous AN/$LiClO_4$ at 500 Hz.

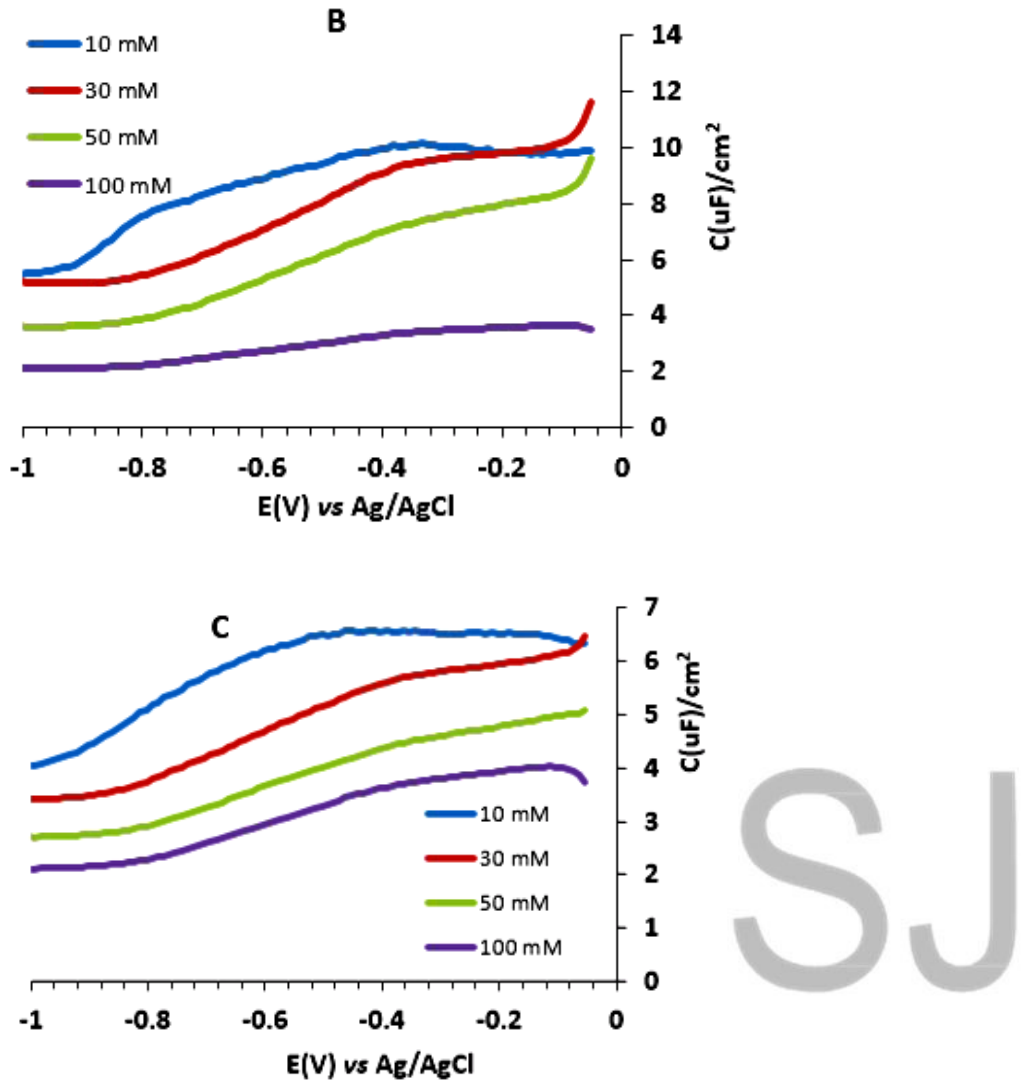

Fig. 9. Capacitance data at Bi in the non-aqueous AN/$LiClO_4$ at (B) 1 kHz (C) 2 kHz

Capacitance measurements at platinum in non-aqueous solvents

For the purpose of comparison, impedance measurements were also carried out with platinum as the working electrode in the non-aqueous electrolyte of acetonitrile/lithium perchlorate. Data obtained from this investigation are presented in figure 10 and as can be observed, values of differential capacitance at this electrode surface in the non-aqueous electrolyte are lower than those obtained at bismuth in the same medium. This is due to the lower relative permittivity of the non-aqueous electrolyte and the much greater tendency for halides to specifically adsorb than perchlorate.

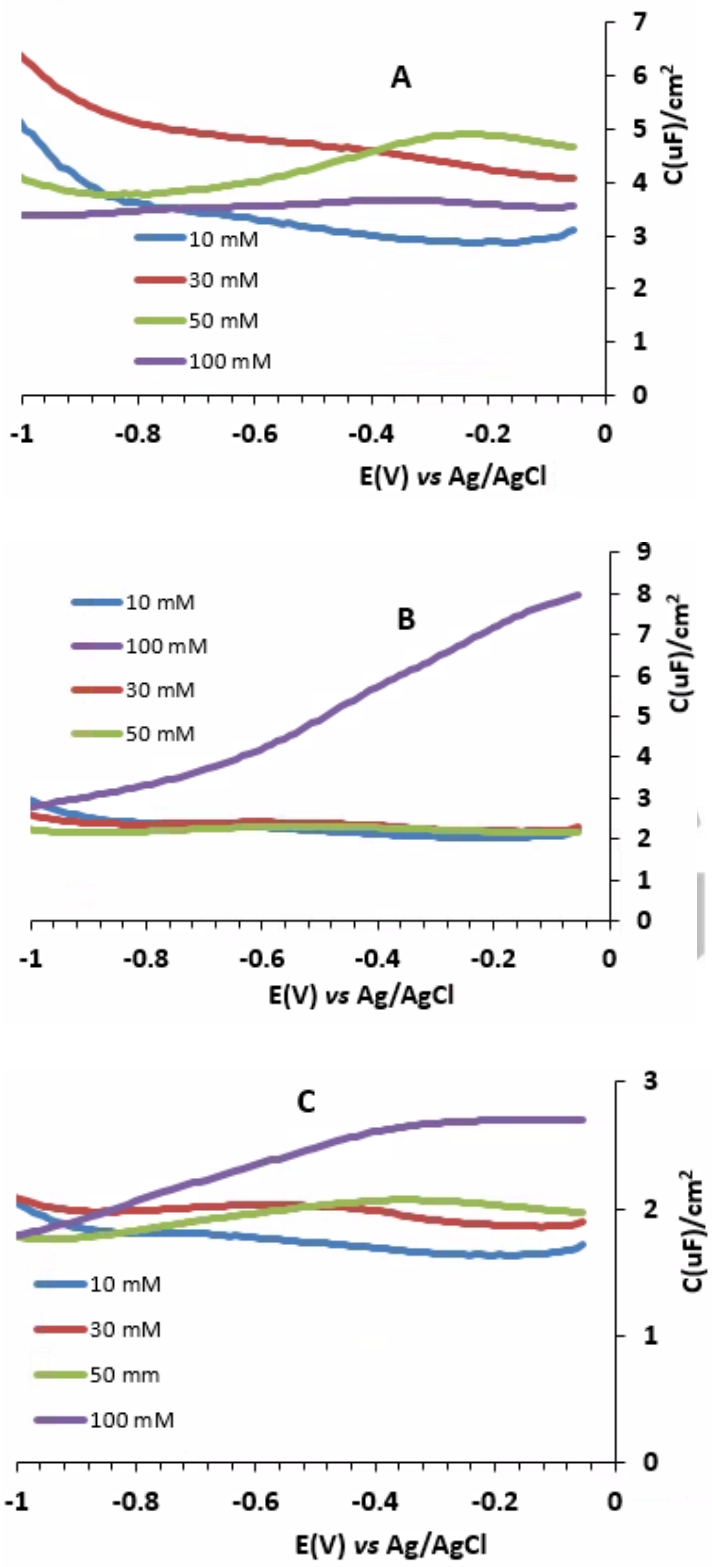

Fig. 10. Capacitance data at Pt in AN/$LiClO_4$ at (A) 500 Hz (B) 1 kHz (C) 2 kHz

This output can be further explained in terms of constant phase element behaviour. The physical roughness of the Bi electrode allows for more adsorption of charges than the relatively smoother surface of the platinum electrode. The sizes of the capacitance values however show a general decrease with increasing magnitude of frequency of measurement, and this is in agreement with theoretical prediction. The unusually high value of differential capacitance recorded in the 100 mM concentration at the frequency of 1 kHz could be attributed to adsorption at the surface associated with high analyte concentrations.

5. Conclusions

Bismuth electrodes have shown complex differential capacitance-potential curves in aqueous electrolytes which are not in line with expectations of the standard double layer theories. The curves generally show a sharp maximum which is suggested to result from pseudocapacitance effects related to the presence of an oxide film at potentials positive of the maximum and its reduction to elemental bismuth at potentials negative of the maximum. Electrochemical impedance spectroscopy (EIS) measurements performed as described in the foregoing sections enabled the determination of potential of zero charge PZC, at the bismuth and platinum electrodes surfaces in two cases. A value of -0.49 V was obtained at bismuth in the aqueous $NaNO_3$/NaCl electrolyte mixture while -0.32 V was the determination made at platinum in aqueous NaBr.

Apart from the 100 mM concentration with higher than 43 µF cm^{-2} effective capacity at 500 Hz, values of double layer capacitance at bismuth for all the other interfaces of NaBr, NaCl and $NaNO_3$ generally fell within the standard range[21, 23] of 10-40 µF cm^{-2}. This implies that the bismuth electrodes can safely replace noble metal electrodes in the measurement of differential capacitance. The high values of differential capacitance recorded in the 100 mM concentration could be attributed to adsorption at the surface associated with high analyte concentrations.

Of electrolyte solutions investigated, double layer capacitance values have shown to increase in the order $LiClO_4$<$NaNO_3$<NaCl<NaBr. In principle the capacitance is expected to increase as the solvated ionic radius decreases. However anions, such as Br^-, which have a strong tendency to specifically adsorb (i.e., lose part of their solvation shell) may not follow this simple trend.

Findings from EIS and XPS experiments put together indicate that the capacitance peaks at bismuth in aqueous solutions are due to adsorption of anions as well as pseudocapacitance contributions of the redox processes of the bismuth oxide film and the metal at this electrode surface. On the other hand, the low values of double layer capacitance (<20 μF cm^{-2}) in the non-aqueous electrolyte of AN/$LiClO_4$ is as a result of the relatively low dielectric constant of AN as well as the weak adsorption capacity of the ClO_4^- anion. This finding is broadly consistent with the Gouy-Chapman-Stern theory.

Acknowledgements: The authors are thankful to the Nigerian Tertiary Education Trust Fund (TetFund) for funding and the University of Newcastle upon Tyne, UK for the provision of equipment and facilities to carry out the research.

Conflict of interests: None.

6. References

1. A. Economou, *Trends in Analytical Chemistry*, 2005, **24**.
2. J. B. Jaimez, M. R. Joya and J. B. Ortega, *Journa of Physics : Conference series 466*, 2013, DOI: 10.1088/1742-6596/466/1/012025, 1-4.
3. P. Jothimuthu, R. A. Wilson, J. Herren, E. N. Haynes, W. R. Heineman and I. Papautsky, *Biomed Microdevices*, 2011, **13**, 695-703.
4. V. Rehacek, I. Hotovy, M. Vojs and F. Mika, *Microsyst Technol*, 2008, **14**, 491-498.
5. I. Scanvara, C. Prior, S. B. Hocevar and J. Wang, *Electroanalysis*, 2010, **22**, 1405-1420.
6. J. Wang, *Electroanalysis*, 2005, **17**, 1341-1346.
7. J. Wang, J. Lu, U. A. Kirgoz, S. B. Hocevar and B. Ogorevc, *Analytica Chimica Acta*, 2001, **434**, 29-34.
8. Z. Zou, A. Jang, E. MacKnight, P. Wu, J. Do, P. L. Bishop and C. H. Ahn, *Sensors and Actuators B: Chemical*, 2008, **134**, 18-24.
9. J. Wang and J. Lu, *Electrochemistry Communications*, 2000, **2**, 390-393.
10. J. Wang, J. Lu, S. B. Hocevar, P. A. M. Farias and B. Ogorevc, *Analytical Chemistry.*, 2000, **72**, 3218-3222.
11. E. Härk and E. Lust, *Journal of The Electrochemical Society*, 2006, **153**, 7.
12. R. Pauliukaitė, S. B. Hočevar, B. Ogorevc and J. Wang, *Electroanalysis*, 2004, **16**, 719-723.
13. M. Vaartnou and E. Lust, *J Solid State Electrochem*, 2014, 173-180.
14. S. Dal Borgo, V. Jovanovski, B. Pihlar and S. B. Hocevar, *Electrochimica Acta*, 2015, **155**, 196-200.
15. E. A. Hutton, B. Ogorevc, S. B. Hocevar, F. Weldon, M. R. Smith and J. Wang, *Electrochemistry Communications*, 2001, **3**, 707-711.
16. É. S. Sá, P. S. da Silva, C. L. Jost and A. Spinelli, *Sensors and Actuators B: Chemical*, 2015, **209**, 423-430.

17. N. Serrano, A. Alberich, J. M. Diaz-Cruz, C. Arino and M. Esteben, *Trends in Analytical Chemistry*, 2013, **46**, 15-29.
18. R. T. Isaacson and G. A. Williams, *Physical Review*, 1969, **185**, 682-688.
19. S. K. Cook and B. R. Horrocks, *ChemElectroChem*, 2016, **3**, 1-13.
20. G. E. Smith, G. A. Baraff and J. M. Rowell, *Physical Review*, 1964, **135**, A1118-A1124.
21. A. J. Bard and L. R. Faulkner, *Electrochemical Methods: Fundamentals and Applications.*, John Wiley and Sons., New York, 2nd edn., 2001.
22. C. M. Brett and A. M. O. Brett, *Electrochemistry. Principles, Methods and Applications.*, Oxford University Press., New York, 1994.
23. J. Wang, *Analytical Electrochemistry.*, VCH Publishers., New York, 1994.
24. K. Lust, M. Vaartnou and E. Lust, *Electrochimica Acta*, 2000.
25. K. Lust, M. Vaartnou and E. Lust, *Journal of Electroanalytical Chemistry*, 2002, **532**.
26. J. F. McGilp, P. Weighton and E. J. McGuire, *Journa of Physics C: Solid State Physics*, 1977, **10**, 3445-3460.
27. L. Ley, S. P. Kowalczyk, F. R. McFeely, R. A. Pollak and D. A. Shirley, *Physical Review B*, 1973, **8**, 2392-2402.
28. W. E. Morgan, J. R. V. Wazer and W. J. Stec, *Journal of American Chemical Society*, 1973, **95**, 751-755.
29. P. M. Th M. van Attekum and J. M. Trooster., *Physical Review B*, 1979, **20**, 2335-2340.
30. P. S. A. Kumar, S. Mahamumi, A. S. Nigaveka and S. K. Kulkarmi, *Physica C*, 1992, **201**, 145-150.
31. C. J. Powell., *Journal of Electron Spectroscopy and Related Phenomena*, 2012, **185**, 1-3.
32. R. B. Shalvoy, G. B. Fisher and P. J. Stiles., *Physical Review B*, 1977, **15**, 1680-1697.
33. R. Nyholm, A. Berndtsson and N. Martensson, *Journal of Physics C: Solid State Physics*, 1980, **13**, L1091-L1096.
34. V. S. Dharmadhikari, S. R. Sainkar, S. Badrinarayan and A. Goswami, *Journal of Electron Spectroscopy and Related Phenomena.*, 1982, **25**, 181-189.
35. B. Afsin and M. W. Roberts, *Spectroscopy Letters*, 1994, **1**.
36. V. I. Nefedov and Y. V. Salyn, *Journal of Electron Spectroscopy and Related Phenomena.*, 1977, **10**.
37. T. P. Debies and J. W. Rabalais, *Chemical Physics.*, 1977, **20**, 277-283.
38. W. E. Morgan, W. J. Stec and J. R. V. Wazer, *Inorganic Chemistry*, 1973, **12**, 953-955.
39. Y. Schuhl, H. Baussart, R. Delobel, M. L. Brass, J. Leroy, L. G. Gengembre and J. Grimblot, *Journal of Chemical Society. Faraday Transaction I.*, 1983, **79**, 2055-2069.
40. A. S. Nomor and B. R. Horrocks., *ChemElectroChem*, 2017, **4**, 2943-2951.
41. J. A. Riddick, W. B. Bunger and T. K. Sakano., *Organic Solvents: Physical Properties and Methods of Purification*, Wiley-Interscience, New York, 4th edn., 1986.
42. M. Vaartnou and E. Lust, *J. Electroanal. Chem.*, 2002, **533**.